Surface Origin of High Conductivities in Undoped In_2O_3 Thin Films

S. Lany,[1] A. Zakutayev,[1] T. O. Mason,[2] J. F. Wager,[3] K. R. Poeppelmeier,[2] J. D. Perkins,[1] J. J. Berry,[1] D. S. Ginley,[1] and A. Zunger[4]

[1]*National Renewable Energy Laboratory, Golden, Colorado 80401, USA*
[2]*Northwestern University, Evanston, Illinois 60208, USA*
[3]*Oregon State University, Corvallis, Oregon 97331, USA*
[4]*University of Colorado, Boulder, Colorado 80309, USA*

(Received 6 August 2011; published 5 January 2012)

The microscopic cause of conductivity in transparent conducting oxides like ZnO, In_2O_3, and SnO_2 is generally considered to be a point defect mechanism in the bulk, involving intrinsic lattice defects, extrinsic dopants, or unintentional impurities like hydrogen. We confirm here that the defect theory for O-vacancies can quantitatively account for the rather moderate conductivity and off-stoichiometry observed in bulk In_2O_3 samples under high-temperature equilibrium conditions. However, nominally undoped thin-films of In_2O_3 can exhibit surprisingly high conductivities exceeding by 4–5 orders of magnitude that of bulk samples under identical conditions (temperature and O_2 partial pressure). Employing surface calculations and thickness-dependent Hall measurements, we demonstrate that surface donors rather than bulk defects dominate the conductivity of In_2O_3 thin films.

DOI: 10.1103/PhysRevLett.108.016802 PACS numbers: 73.20.−r, 72.20.−i, 71.20.−b

Functional oxides in optoelectronic applications are today most commonly employed in the thin-film form [1,2]. One class of such thin-film materials that is important in solar energy conversion and other technologies are the transparent conducting oxides (TCO) which exhibit the often contradictory coexistence of high conductivity and optical transparency [2]. In many applications, the desired high conductivities of TCO are achieved through addition of extrinsic dopants like, e.g., Sn_{In} in In_2O_3 [3–5]. However, the TCO prototype oxides, ZnO, In_2O_3, and SnO_2 exhibit considerable *n*-type conductivity even in the absence of intentional doping [1], which has stirred significant interest towards the microscopic origin of the electron carriers. The explanations for such intrinsic conductivity that have been offered so far are mostly based on bulk defect models, involving intrinsic defects like O vacancies [5–10], unintentional impurities like hydrogen [11,12], or defect complexes [13,14]. For bulk In_2O_3, we validate the traditional point defect mechanism of O-vacancy formation by a quantitative comparison of experimental literature data for high-temperature equilibrium conditions [7,15] with predictions from defect theory. At the same time, we demonstrate that such bulk models cannot account for the fact that thin-film conductivities can be 4–5 orders of magnitude higher, and reach TCO-like conductivities above 1000 S/cm in pure In_2O_3 thin films [1]. Since, on the other hand, it is well known that surface defects play an important role in many oxide applications, like catalysis [16,17], we investigate here the possibility that surface defects are the cause of conductivity in thin-film TCO. To this end, we performed surface calculations and thickness-dependent Hall measurements in epitaxial In_2O_3 films, finding that (i) the formation energies of electron-producing intrinsic surface donors is much lower than that of their bulk counterparts, and (ii) that the surface carrier sheet density dominates the conductivity of epitaxial films up to about 150 nm thickness. Thus, we conclude that the conductivity of In_2O_3 thin films is decisively controlled by surface defects instead of the traditional bulk defect mechanism. This finding implies that oxides which are nonconductive or even nondopable as bulk materials can nevertheless become highly conductive as thin films.

Oxygen vacancy formation and ionization.—The two central quantities discussed here for In_2O_3, the O-deficient nonstoichiometry and the generation of free electrons, are often associated with the (equilibrium) formation of oxygen vacancies [6]

$$O_O \rightleftharpoons V_O^0 + \frac{1}{2} O_2, \tag{1}$$

followed by the thermal ionization of the V_O double donors,

$$V_O^0 \rightleftharpoons V_O^{2+} + 2e. \tag{2}$$

The enthalpy $\Delta H[V_O]$ of vacancy formation [cf. Eq. (1)] depends on the chemical potential of oxygen, which we define relative to the energy of an O atom in the O_2 molecule, as $\Delta\mu_O = \mu_O - 1/2E(O_2)$. In equilibrium, the chemical potentials $\Delta\mu_O$ of oxygen and $\Delta\mu_{In}$ of In are mutually dependent and obey the relationship

$$2\Delta\mu_{In} + 3\Delta\mu_O = \Delta H_f(In_2O_3), \tag{3}$$

where $\Delta H_f = -9.6$ eV is the heat of formation of In_2O_3 [18]. Thus, under maximally reducing (In-rich—O-poor) conditions the chemical potentials are $\Delta\mu_{In} = 0$, and

$\Delta\mu_O = -3.2$ eV [cf. Eq. (3)]. For more oxidizing (In-poor—O-rich) conditions, $\Delta\mu_O$ is determined as a function of the temperature T and the partial pressure pO_2 via the ideal gas law [5]. The release of free electrons, Eq. (2), depends on the donor transition energy $\varepsilon(2+/0)$ (ionization energy) and on the Fermi energy E_F. In order to predict the concentrations of O vacancies and free carriers as a function of T and pO_2, we use a thermodynamic model where we solve numerically a self-consistency condition for the formation energy $\Delta H[V_O]$, the defect concentration, and the Fermi level E_F under the constraint of overall charge neutrality [19].

Bulk In_2O_3.—Figure 1 shows the predicted V_O concentrations and carrier densities based on our earlier supercell calculations for the formation energies of intrinsic defects in In_2O_3 [5], where we have now taken into account the recent reassignment of the band-gap energy of In_2O_3 ($E_g = 3.1$ eV at low temperature [20]) and the results of many-body quasiparticle energy calculations [10,21] which predict a rather large ionization energy for V_O in In_2O_3, i.e., $\varepsilon(2+/0) = E_{CBM} - 0.7$ eV (see also *Methods* below and Supplemental Material [22]). While such a deep donor level implies that O vacancies will not lead to significant conductivity under ambient conditions (except, possibly, through the persistent photoconductivity mechanism [5]), the temperature-induced band-gap reduction of In_2O_3 of about 1 meV/K [15] decreases the separation energy between the donor level and the conduction band minimum (CBM), thereby leading to a more effective ionization at the high temperatures needed for thermal (equilibrium) generation of O vacancies. For example, we obtain a predicted electron density of $n = 10^{16}$ cm^{-3} at $T = 1000$ K [Fig. 1(a)], which is in good agreement with the corresponding experimental conductivity, $\sigma = 0.01$ S/cm [7], considering that the respective mobility is in the order of 10 cm^2/Vs [6]. The temperature dependence of n exhibits an Arrhenius behavior between 750 and 1500 K with an activation energy of $E_a = 1.8$ eV [Fig. 1(a)], consistent with experimental observations ($E_a = 1.5$–1.6 eV [7,15]). The calculated V_O concentration as a function of pO_2 at $T = 1073$ K, shown in Fig. 1(b), follows the expected [6] power law with an exponent of $-1/6$ under all but the most reducing conditions [23]. The calculated off-stoichiometry parameter δ agrees well (within a factor of 2) with thermogravimetric measurements which have been reported between $\log[pO_2/\text{atm}] = -5$ and -15 at the same temperature [24]. Thus, theory consistently explains the experimental conductivity and off-stoichiometry of pure bulk In_2O_3 in equilibrium with the O_2 gas phase at elevated temperatures.

Thin-film In_2O_3.—Experimentally, one routinely observes in polycrystalline undoped In_2O_3 thin films conductivities above 1000 S/cm, corresponding to carrier densities in the 10^{20}–10^{21} cm^{-3} range [1]. The source of this "intrinsic" thin-film conductivity is unknown. Figure 2 shows the measured conductivity as a function of pO_2 at 859 K for a 320 nm thick sputter-deposited polycrystalline In_2O_3 thin film [25]. The power law behavior with a $-1/6$ exponent and the reversibility of the measurement shown in Fig. 2 point toward an equilibrium defect formation mechanism such as vacancy generation according to Eqs. (1) and (2). The puzzle is, however, that the thin-film conductivities are about 4 orders of magnitude larger than the bulk defect model can explain under the respective conditions. For example, the thin-film conductivity is $\sigma_{TF} = 35$ S/cm at $T = 859$ K and $pO_2 = 0.2$ atm (see Fig. 2), but the conductivity measured in the bulk under these conditions is only $\sigma_{bk} = 10^{-3}$ S/cm [7]. Also, the corresponding carrier densities around $n_{TF} = 10^{19}$ cm^{-3} in the thin film are much larger than what could be associated with the thermal generation of O vacancies ($n_{bk} = 3 \times 10^{14}$ cm^{-3} at 859 K, see Fig. 1). Indeed, when we extrapolate the $-1/6$ power law to maximally reducing conditions [i.e., the In-rich—O-poor limit, cf. Eq. (3)], we obtain an extremely high conductivity of $\sigma_{TF} = 10^6$ S/cm. The corresponding carrier and defect densities around 10^{24} cm^{-3} exceed the number of available lattice sites, implying unphysical negative formation energies under the In-rich condition. Therefore, we rule out a bulk point defect mechanism as the cause of the higher thin-film conductivity compared to bulk samples.

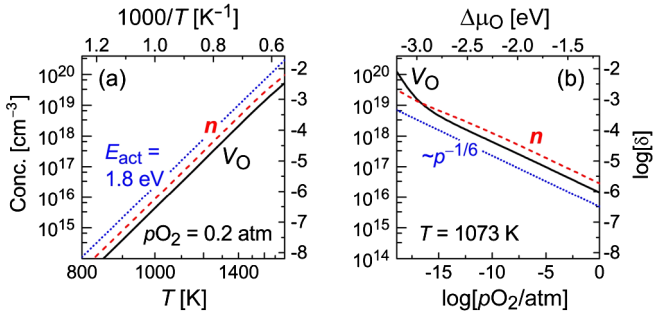

FIG. 1 (color online). Calculated equilibrium concentrations of O vacancies (V_O) and electron densities n in undoped In_2O_3 as function of (a) the temperature and (b) the O_2 partial pressure.

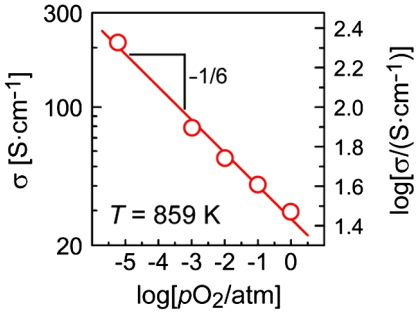

FIG. 2 (color online). Steady state conductivity as a function of pO_2 of an In_2O_3 thin film at 859 K sample temperature [25]. The solid line shows the power law with an exponent of $-1/6$.

Intrinsic surface donors.—For the surface calculations (see below for details on the employed methods), we consider the particularly stable (111) surface orientation of In_2O_3 which—due to faceting—occurs even after epitaxial growth on different substrate orientations [26]. The surface energy is calculated as 50 meV/Å^2. The calculated ionization potential (IP) is 6.8 eV, as compared to a range 7.0–7.6 eV measured in photoemission experiments [27], where the larger values have been attributed to adsorbed surface species. As shown in Fig. 3, the surface band gap is reduced to 2.3 eV, down from 3.1 eV in the bulk, due to an offset of 0.2 eV between the surface and bulk CBM, and an offset of 0.6 eV between and the surface and bulk valence band maxima. The unoccupied conduction bandlike surface states are localized only in the direction perpendicular to the surface, but have a considerable dispersion along in-plane directions. Thus electrons released into the surface conduction band cause a 2D conductive layer.

Figure 3 shows the calculated single-particle energies for the electronic states introduced by an In adatom $In_{ad}^{(111)}$ and by a surface O vacancy $V_O^{(111)}$, which are the surface counterparts of the In_i and V_O defects in the bulk. As seen in Fig. 4a, the In adatom creates a doubly occupied state deep inside the surface band gap which is nonconductive, but also a singly occupied shallow conductive state that is derived from the surface conduction band. The surface vacancy $V_O^{(111)}$ creates a doubly occupied state which lies considerably higher in energy than the respective states of the O vacancy in the bulk. Since its energy is practically degenerate with the surface CBM (Fig. 3), the electrons can easily be thermally excited into the (surface or bulk) conduction band at room temperature, thereby causing conductivity.

Figure 4 shows the formation energies of the charge-neutral $In_{ad}^{(111)}$ and $V_O^{(111)}$ surface donors as a function of pO_2 at $T = 1023$ K. Compared to the respective bulk defects, the formation energies are much reduced, e.g., $\Delta H[V_O^{(111)}]$ is 1.4 eV lower than $\Delta H[V_O^{(bulk)}]$. (The V_O formation energy shown in Fig. 4 is the lowest found among the 4 inequivalent O sites in the first O layer.) A similar reduction has recently been reported in Ref. [28]. Whereas ΔH of the bulk defects stays positive throughout the full range of chemical potentials, the surface defect formation energies become negative at low O_2 partial pressures around $pO_2 = 10^{-10}$ atm (see Fig. 4), indicating that under such reducing conditions the excessive surface defect formation induces a nonstoichiometric (In-excess—O-deficient) reconstruction. Under less reducing conditions, the formation energies are still low enough, e.g., $\Delta H[V_O^{(111)}] < 1.1$ eV below pO_2 in air, to afford large sheet densities of surface donors. Thus, we conclude that the formation of intrinsic surface donors is a likely source of the recently reported electron accumulation at the surface of In_2O_3 [20].

Surface vs bulk contributions to the carrier density.—In order to examine the hypothesis that the thin-film conductivity is determined by surface defects, we performed Hall measurements of In_2O_3 thin films as a function of the film thickness, shown in Fig. 5(a). For this purpose, we have grown In_2O_3 thin films epitaxially on yttria stabilized zirconia (YSZ) substrates. The total carrier density $n_{tot} = \eta_{tot}/d$, i.e., the measured sheet carrier density η_{tot} of the entire film divided by the film thickness d, is analyzed using a two-component model,

$$n_{tot} = n_b + \eta_s/d, \tag{4}$$

which includes a bulklike component n_b due to carriers originating from donor defects in the film interior, and a surface component due to the sheet carrier density η_s created by surface donors. The resulting values of n_b and η_s for (111) oriented films are shown in Table I. We find that in these epitaxial films, the surface component η_s/d dominates the electrical properties (i.e., $\eta_s/d > n_b$) up to a thickness of $d = 150$ nm. In polycrystalline films

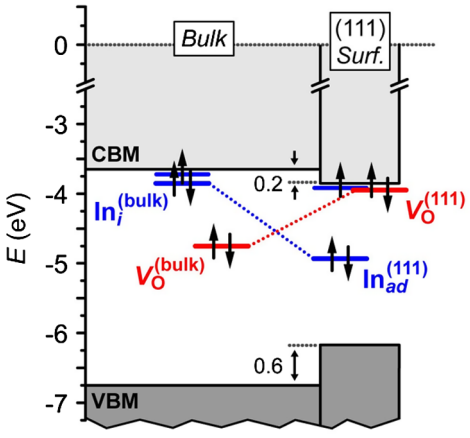

FIG. 3 (color online). Band diagram for bulk In_2O_3 and the stoichiometric (111) surface, showing the energy positions of the occupied single-particle states created by bulk point defects In_i and V_O, and by $In_{ad}^{(111)}$ and $V_O^{(111)}$ at the surface.

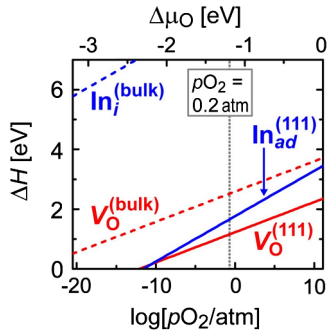

FIG. 4 (color online). Formation energies ΔH of the charge-neutral intrinsic (surface and bulk) donors in In_2O_3 as a function of the oxygen chemical potential $\Delta\mu_O$ and the respective partial pressure pO_2 for $T = 1023$ K.

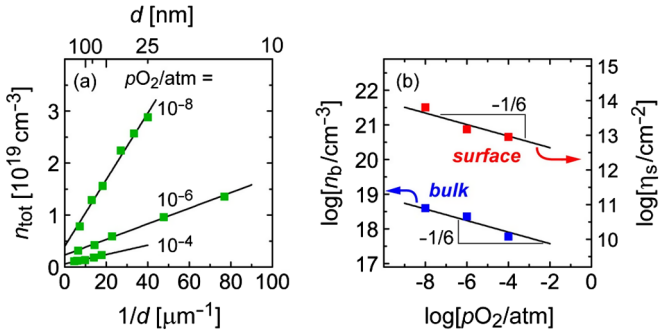

FIG. 5 (color online). (a) Total carrier concentration of In_2O_3 (111) epitaxial thin films grown at $T = 1023$ K under pO_2 between 10^{-8} and 10^{-4} atm as a function of the reciprocal film thickness $1/d$. (b) The pO_2 dependence of both the film-interior (n_b) and surface (η_s) components. The $-1/6$ slopes are shown as a guide to the eye.

(cf. Fig. 2), the surface component can be expected to be even more important, because the presence of internal porosity of grain boundaries would be expected to increase the effective surface area. Indeed, the conductivity of the polycrystalline film (Fig. 2) is more that an order of magnitude higher than that of an epitaxial film (Fig. 5) of the same thickness.

Plotting the film interior (n_b) and surface (η_s) components as a function of the O partial pressure during thin-film growth [Fig. 5(b)], we find that both components can be described by the power law behavior with the $-1/6$ exponent. The crucial conclusion is that the observation of this exponent in thin films, e.g., in Fig. 2, is not a unique signature of the traditional point defect mechanism described by Eqs. (1) and (2), but instead points also towards a surface-dominated conductivity.

Conclusions.—The microscopic cause of conductivity in TCO has been a long standing topic of discussion and debate, which has so far focused mostly on defects, dopants, and impurities in the bulk, including traditional donor doping through higher valent elements [3–5], intrinsic defects (interstitials and vacancies) [5,6,8–10], and hydrogen incorporation [11,12]. We emphasized here that such bulk defect models are incapable to account for the high carrier densities above 10^{20} cm^{-1} that are observed in nominally undoped In_2O_3 when it is grown in the technologically important thin-film form. The formation energies of intrinsic defects or hydrogen impurities are too high to account for such high electron concentrations [29], and the donor level of O vacancies is too deep to produce large densities of free electrons at room temperature [10]. Instead, we showed here in a combined theoretical and experimental study that such bulk effects are overshadowed by carriers caused by surface donors, thereby resolving the puzzle of mysteriously high carrier densities in undoped In_2O_3 thin films. This finding highlights a fundamental difference between TCO materials in the bulk and thin-film forms, and could lead to new approaches for the design of optoelectronic devices with TCO thin films as the conducting contact layer.

TABLE I. Bulk carrier densities n_b and (111) surface carrier sheet densities η_s of epitaxial In_2O_3 thin films grown at $T = 1023$ K.

	n_b(cm^{-3})	η_s(cm^{-2})
$pO_2 = 10^{-8}$ atm	$4.0(8) \times 10^{18}$	$6.4(3) \times 10^{13}$
$pO_2 = 10^{-6}$ atm	$2.3(2) \times 10^{18}$	$1.5(1) \times 10^{13}$
$pO_2 = 10^{-4}$ atm	$0.6(1) \times 10^{18}$	$0.9(1) \times 10^{13}$
Atomic site density	7.7×10^{22}	1.6×10^{15}

Methods.—The electronic structure calculations in this work were performed within the projector-augmented plane-wave pseudopotential formalism implemented in the VASP code [30]. Total energies were calculated within the generalized gradient approximation of Ref. [31], and defect formation energies were determined by supercell calculations including band-gap and image charge corrections as described in Ref. [32]. Compared to our earlier results for bulk defects in In_2O_3 [5], we here considered the revised band-gap energy of In_2O_3 [20], the results of *GW* quasiparticle energy calculations [10,21], and corrections for the elemental energies that yield the calculated heats of formation close to experiment [33]. For the surface calculations we used a supercell slab with 240 atoms. For the calculation of the (surface) band structure and energies of the donor states (Fig. 4), it is necessary to perform a band-gap corrected calculation. Thus, we employed nonlocal external potentials [34] (V_{nlep}), which were fitted to reproduce both the *GW* band gap and the position of the V_O defect level in bulk In_2O_3. Further information about the surface supercell construction and the empirical potentials is given in the Supplemental Material [22].

The conductivity data shown in Fig. 2 was measured by the van der Pauw method on a 320 nm thick polycrystalline In_2O_3 thin film that was grown by sputter deposition at 673 K on a MgO single crystal substrate [25]. The epitaxial In_2O_3 thin films (data shown in Fig. 5) were grown by pulsed laser deposition and subsequently characterized under ambient conditions. The thickness of the samples was measured using profilometry, and the sheet carrier density was determined from resistivity and Hall effect measurements in Van der Pauw geometry. A roughness of approximately 1 nm was determined from atomic force microscopy.

This work is supported by the U.S. Department of Energy, Office of Science, Office of Basic Energy Sciences under Contract No. DE-AC36-08GO28308 to NREL. The "Center for Inverse Design" is a DOE Energy Frontier Research Center. The use of MPP capabilities at the National Energy Research Scientific Computing Center is gratefully acknowledged. We thank C. Körber, S. P. Harvey, and A. Klein for providing their

unpublished In_2O_3 thin-film data. We thank A. R. Nagaraja and N. H. Perry for confirming the conductivity range of 1–10 S/cm for bulk In_2O_3 by performing conductivity measurements on air-annealed/quenched samples; we thank Y. Ke and P. A. Parialla for their assistance with x-ray diffraction measurements and interpretation; we thank A. G. Norman and K. M. Jones for the supporting TEM measurements and sample preparation; we thank A. K. Sigdel for his help with atomic force microscopy measurements.

[1] H. L. Hartnagel, A. L. Dawar, A. K. Jain, and C. Jagadish, *Semiconducting Transparent Thin Films* (IOP Publishing, Bristol, 1995).
[2] *Transparent Conducting Oxides*, edited by D. S. Ginley and C. Bright (MRS Bulletin, Warrendale, PA, 2000), Vol. 25.
[3] G. Frank and A. Köstlin, Appl. Phys. A **27**, 197 (1982).
[4] G. B. González, T. O. Mason, J. P. Quintana, O. Warschkow, D. E. Ellis, J. H. Hwang, J. P. Hodges, and J. D. Jorgensen, J. Appl. Phys. **96**, 3912 (2004).
[5] S. Lany and A. Zunger, Phys. Rev. Lett. **98**, 045501 (2007).
[6] F. A. Kröger, *The Chemistry of Imperfect Crystals* (North-Holland, Amsterdam, 1974), 2nd ed.
[7] J. H. W. de Wit, J. Solid State Chem. **13**, 192 (1975); J. H. W. de Wit, G. van Unen, and M. Lahey, J. Phys. Chem. Solids **38**, 819 (1977).
[8] A. Ambrosini, G. B. Palmer, A. Maignan, K. R. Poeppelmeier, M. A. Lane, P. Brazis, C. R. Kannewurf, T. Hogan, and T. O. Mason, Chem. Mater. **14**, 52 (2002).
[9] P. Agoston, K. Albe, R. M. Nieminen, and M. J. Puska, Phys. Rev. Lett. **103**, 245503 (2009).
[10] S. Lany and A. Zunger, Phys. Rev. Lett. **106**, 069601 (2011); P. Agoston, K. Albe, R. M. Nieminen, and M. J. Puska, Phys. Rev. Lett. **106**, 069602 (2011).
[11] C. G. van de Walle, Phys. Rev. Lett. **85**, 1012 (2000).
[12] S. Limpijumnong, P. Reunchan, A. Janotti, and C. G. van de Walle, Phys. Rev. B **80**, 193202 (2009).
[13] D. C. Look, G. C. Farlow, P. Reunchan, S. Limpijumnong, S. B. Zhang, and K. Nordlund, Phys. Rev. Lett. **95**, 225502 (2005).
[14] Y. S. Kim and C. H. Park, Phys. Rev. Lett. **102**, 086403 (2009).
[15] R. L Weiher, J. Appl. Phys. **33**, 2834 (1962); R. L Weiher and B. G. Dick, J. Appl. Phys. **35**, 3511 (1964).
[16] U. Diebold, J. Lehman, T. Mahmoud, M. Kuhn, G. Leonardelli, W. Hebenstreit, M. Schmid, and P. Varga, Surf. Sci. **411**, 137 (1998).
[17] R. Schaub, P. Thostrup, N. Lopez, E. Lægsgaard, I. Stensgaard, J. K. Nørskov, and F. Besenbacher, Phys. Rev. Lett. **87**, 266104 (2001).
[18] D. D. Wagman *et al.*, The NBS tables of chemical thermodynamic properties, J. Phys. Chem. Ref. Data 11, Supp. 2, (1982).
[19] S. Lany, Y. J. Zhao, C. Persson, and A. Zunger, Appl. Phys. Lett. **86**, 042109 (2005).
[20] P. D. C. King, T. D. Veal, F. Fuchs, Ch. Y. Wang, D. J. Payne, A. Bourlange, H. Zhang, G. R. Bell, V. Cimalla, O. Ambacher, R. G. Egdell, F. Bechstedt, and C. F. McConville, Phys. Rev. B **79**, 205211 (2009).
[21] S. Lany and A. Zunger, Phys. Rev. B **81**, 113201 (2010).
[22] See Supplemental Material at http://link.aps.org/supplemental/10.1103/PhysRevLett.108.016802 for details on the slab supercell calculations and band gap corrections.
[23] At very low values of $\Delta\mu_O$, the incomplete ionization of the formed vacancies [cf. Eq. (2)] leads to a deviation from the power law. It should also be noted here that In interstitial defects, which would yield a similar $-3/16$ exponent, have been excluded on energetic grounds [5].
[24] R. Dieckmann, Ceramic Transactions **71**, 33 (1996).
[25] C. Körber, S. P. Harvey, T. O. Mason, and A. Klein (unpublished).
[26] E. H. Morales, Y. He, M. Vinnichenko, B. Delley, and U. Diebold, New J. Phys. **10**, 125030 (2008).
[27] S. P. Harvey, T. O. Mason, C. Körber, Y. Gassenbauer, and A. Klein, Appl. Phys. Lett. **92**, 252106 (2008).
[28] A. Walsh, Appl. Phys. Lett. **98**, 261910 (2011).
[29] Even though the hydrogen interstitial (H_i) is a relatively low energy defect in In_2O_3 [12], carrier densities above 10^{20} cm^{-3} are difficult to explain by equilibrium incorporation of H_i, since the reduction of the H chemical potential μ_H relative to $1/2E(H_2)$ under realistic conditions increases the H_i formation energy (e.g., $\Delta\mu_H = -0.7$ eV at $T = 1000$ K and $pH_2 = 1$ atm).
[30] G. Kresse and D. Joubert, Phys. Rev. B **59**, 1758 (1999).
[31] J. P. Perdew, K. Burke, and M. Ernzerhof, Phys. Rev. Lett. **77**, 3865 (1996).
[32] S. Lany and A. Zunger, Phys. Rev. B **78**, 235104 (2008).
[33] S. Lany, Phys. Rev. B **78**, 245207 (2008).
[34] S. Lany, H. Raebiger, and A. Zunger, Phys. Rev. B **77**, 241201(R) (2008).